4.1 DESIGN AND DEVELOPMENT OF NOVEL COPPER ALLOYS FOR FUSION ENERGY APPLICATIONS—Ying Yang (Oak Ridge National Laboratory) and Steven J. Zinkle (University of Tennessee and Oak Ridge National Lab)

OBJECTIVE

This study aims at developing high strength, high conductivity Cu alloys with improved thermal creep strength for long pulse fusion high heat flux structures. It uses an accelerated approach of computational thermodynamics guided alloy design.

SUMMARY

A computation thermodynamics tool for designing and developing Cu-Cr-Nb-Zr alloys have been successfully developed. Thermodynamic modeling results based on this tool enabled a rapid development of a novel CuCrNbZr alloys with targeted microstructure using an economical, conventional ingot making method following by simple heat treatment procedures. The new alloys display uniform grain structure with bimodal distribution of precipitates.

PROGRESS AND STATUS

Introduction

High strength, high conductivity copper alloys are a potentially attractive option for the high heat flux structure in fusion energy systems. They are being utilized in ITER, and are under consideration for next step devices in Europe and elsewhere [1]. The conventional approach to produce high strength, high conductivity copper alloys uses fine-scale particles (either precipitates produced by solution anneal and aging, or inert dispersoids such as fine-scale oxides produced by powder metallurgy approaches). The optimized strength and conductivity near room temperature for copper alloys is typically achieved by introducing a small volume fraction ((f~1-5%) of uniformly dispersed nanoscale (diameter ~3-10 nm) precipitates or dispersoids [2]. Although impressive room temperature yield strengths of 300-1000 MPa and conductivities 200-360 W/m-K have been achieved in several Cu alloys, all current commercially available high strength, high conductivity Cu alloys suffer significant thermal creep deformation at temperatures above 300-400°C [2]. Since 400°C in Cu is equal to 0.5 T_M (where T_M is the melting temperature), which typically represents the onset of pronounced thermal creep in simple metals due to high atomic mobility, new Cu alloys specifically tailored for thermal creep resistance need to be designed in order to achieve improved strength near or above 400°C. To date, there has been insufficient commercial incentive to develop high performance thermal creep-resistant Cu alloys since most of the current commercial applications for Cu alloys involve operating temperatures near room temperature (high field magnets, resistance spot welding electrodes, chill block molds, air- or water-cooled high heat flux apparatus, etc.)

Approach

Analysis of the thermal creep deformation mechanisms for existing Cu alloys near 400°C suggests it is associated with dislocation (power law) creep and grain boundary sliding creep mechanisms [2]. For the design of improved high-performance radiation-resistant copper alloys at elevated temperatures, three key considerations (in addition to having high strength and conductivity) need to be successfully achieved: 1) thermally stable microstructure up to high temperatures; 2) specifically tailored microstructural features to inhibit the relevant thermal creep deformation mechanism (dislocation creep, grain boundary sliding, etc.) that are stable under neutron irradiation; and 3) sufficient sink strength to enable suitable radiation resistance. The physical metallurgy principles for designing high performance Cu alloys specifically tailored for resistance to thermal creep at elevated temperatures have been outlined by several authors [2-6]. Key design features include utilization of relatively large particles along grain boundaries to inhibit grain boundary movement along with a medium to high density of fine-scale matrix

precipitates that provide resistance to dislocation motion. The fine-scale matrix particles also provide beneficial radiation resistance by promoting recombination of neutron irradiation-induced vacancies and interstitials [7]. For high creep strength, high thermal conductivity and radiation resistance, the optimized matrix particle distribution would consist of a volume particle concentration near f~1-5% with an average particle diameter near 10 nm [2]. The matrix and grain boundary particles must be resistant to thermal and radiation-enhanced coarsening during extended times (>1 year) at intended operating temperatures. It is also desirable (but not required) that the matrix and grain boundary particles be thermally stable during short-term exposure to joining-relevant temperatures (brazing, HIP, etc.).

The design of experimental alloy compositions and heat treatment scheme were aided by computational thermodynamics. The essence of computational thermodynamics, i.e., the CALPHAD (CALculation of PHAse Diagram) approach, was to construct phase diagrams of multicomponent systems based on well assessed thermodynamic functions of Gibbs energy of phases, through a step wise procedure such as binary→ ternary → quaternary. This computational thermodynamic modeling study has been carried out for two quaternary systems, Cu-Cr-Nb-Zr and Cu-Cr-V-Zr.

Cu-Cr-Nb-Zr

The Cu-Cr-Nb-Zr system shows opportunity in forming medium-sized precipitates that pin grain boundary motion involves Cr_2Nb-type laves phase. Although Nb is not a low activation element (desirable for fusion energy applications), our initial efforts are focused on Cu-Cr-Nb-Zr alloys to examine the proof of principle of a newly designed thermal creep resistant alloy that also has good thermal and electrical conductivity and suitable neutron irradiation resistance at 300-450°C.

Computational thermodynamic calculations of Cu-Cr-Nb, Cu-Cr-Zr and Cu-Cr-Nb-Zr alloys have identified several promising compositions and conventional metallurgy processing approaches that should produce a bimodal distribution of large grain boundary particles (e.g., Cu_5Zr or Cr_2Nb laves phase) and a medium to high density of matrix precipitate particles (e.g. Cr or Zr fine scale precipitates) that can be aged to provide good matrix strengthening up to 400-500°C. Based on computational thermodynamic simulation, the new CuCrNbZr alloys were categorized into low Zr and high Zr alloys. Calculation results for low Zr alloys are shown here as an example.

Figure 1 provides a computational thermodynamic simulation on the isothermal phase diagram for the copper alloy within the Cu-Cr-Nb phase space for a constant 0.15 wt% level of Zr. The designed low Zr alloy alloys are located in the phase equilibria of FCC(Cu)+ Bcc(Cr)+Cu_5Zr+Laves_Cr_2(Nb,Zr).

Figure 2(a) provides the full scale plot showing the calculated amount (mole percent) of each phase as a function of temperature for the designed alloy, and Figure 2(b) shows the plot with the enlarged scale from 0 to 3 mole% , for a clear presentation of the amount of precipitate phases. Within the figure are noted the matrix FCC(Cu) phase and the precipitate phases Laves_Cr_2(Nb,Zr), BCC(Cr), Cu_5Zr and $Cu_{51}Zr_{14}$. Figure 2 provides a snapshot of the bimodal type of precipitate distribution, with Laves_Cr_2(Nb,Zr) as the large grain boundary precipitates, and BCC(Cr), Cu_5Zr and $Cu_{51}Zr_{14}$ as the matrix fine scale precipitates.

.

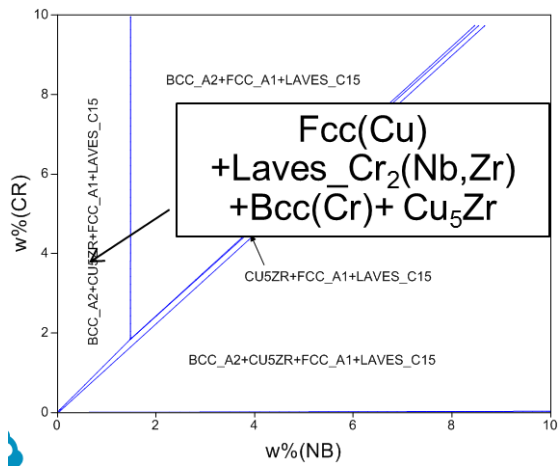

Figure 1. Isothermal section of Cu-Cr-Nb-Zr system at 600°C with a fixed Zr concentration at 0.15 wt%. The designed alloys have a microstructure with a matrix of FCC(Cu) strengthened by various types of precipitates such as Laves_Cr_2(Nb,Zr), Bcc(Cr) and Cu_5Zr.

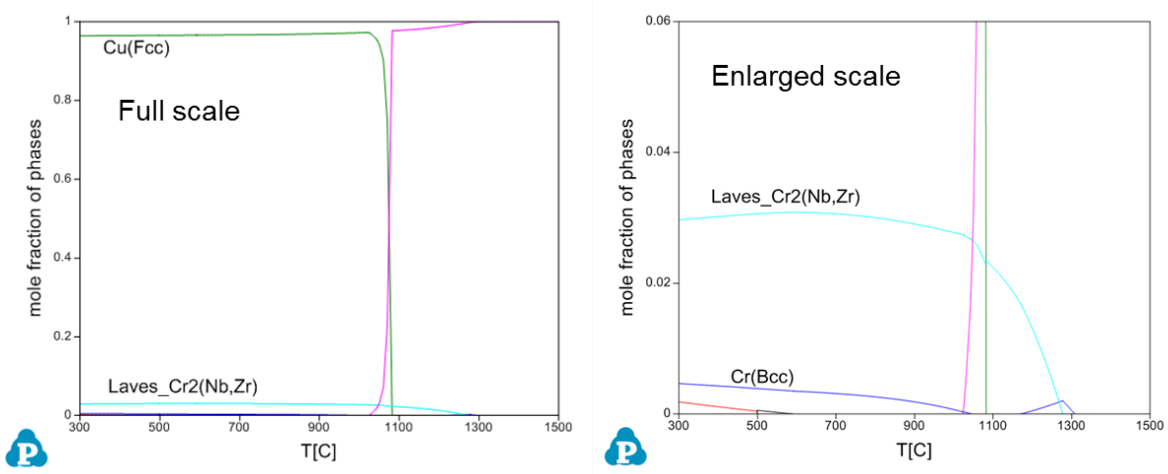

(a) (b)

Figure 2. Calculated mole fraction of phases in the designed alloy as a function of temperature in (a) full and (b) enlarged scale

Cu-Cr-V-Zr

V is a low activation element desirable for fusion energy applications. Therefore, the Cu-Cr-V-Zr was also thermodynamically modeled to explore the potential to form a bimodal distribution of precipitates. However, the modeling results suggested that there is no obvious advantage of V addition into the Cu-Cr-Zr alloys, in terms of precipitate distribution or amount. The same type of microstructure can be realized in the Cu-Cr-Zr ternary alloys. This is due to the lack of new precipitate phase in the Cu-Cr-V system. While in the Cu-Cr-Nb system, there exists the new precipitate Cr_2Nb. Ta and Cr can form the Cr_2Ta laves phase, therefore, Ta might be another element having similar behavior to Nb.

Experimental Procedure

A small ingot of the designed CuCrNbZr alloy was made at ORNL in an argon protected arc-melting furnace followed by drop-casting into the shape of a 0.5x0.5x10 inch rod, with an approximate mass of 100 g. The as-cast rod was then cold rolled at room temperature a total 70% and 50% reduction in thickness. The as-rolled materials were then subjected to various conventional heat treatment schemes,

guided by the computational thermodynamics calculations. The optimum conditions were achieved in CCNZ5A and CCNZ5B alloys with the highest hardness, as shown in Table 1. The conditions without thermal aging are also listed in Table 1 for comparison.

Table 1. Heat treatment conditions and resulting hardness

Sample ID	**Processing (arc-melting and drop cast followed by)**	**Hardness (HV)**
CCNZ5A	Cold roll 70%, solutionized at 970C for 20m, water quench, aging at 475C for 3h, water quench	123.2±1.9
CCNZ5B	Cold roll 50%, solutionized at 970C for 20m, water quench, aging at 475C for 3h, water quench	126.2±7.7
CCNZ6A	Cold roll 70%, solutionized at 970C for 20m, water quench	60.5±3.7
CCNZ6B	Cold roll 50%, solutionized at 970C for 20m, water quench	60.6±0.7

Results

The results in Table 1 suggested that the amount of deformation had negligible effect on hardness, whereas the thermal aging at 475°C following solution quenching was very effective in increasing the alloy strength due to precipitation processes. The typical optical microstructures of samples are shown in Figures 4 (a)~(d), as observed in solution quenched and solution quenched plus aged conditions in the alloy that was initially subjected to 70% deformation. The grain structure with an average grain size of 20 µm was well developed in the thermal aged samples. Fine precipitates on the scale of 50~100 nm were found distributed along grain boundaries and dislocation lines.

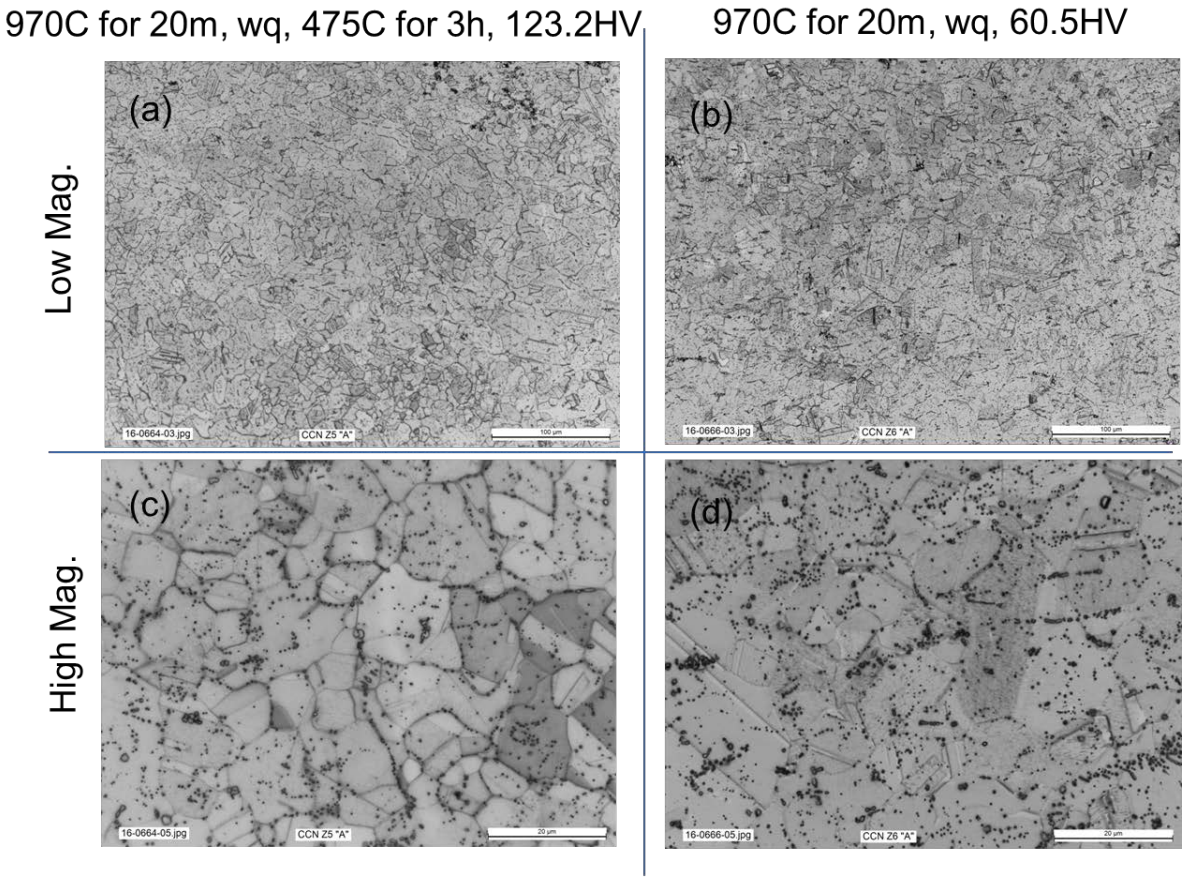

Figure 3. Typical microstructures of samples from the two conditions after 70% deformation.

High resolution of SEM (Scanning Electron Microscopy) BSE (Backscattered Electron) images of samples from CCNZ5A is shown in Figure 4 together with a high magnification optical image. The comparison of the two images in Figure 4 reveals a bimodal distribution of precipitates in the newly designed CuCrNbZr alloy: Cr_2Nb-Laves precipitates (~50-100nm diameter) are distributed at grain boundaries and matrix dislocations, and small Cr (~10nm diameter) precipitates are distributed in the matrix. These ultrafine matrixes Cr precipitates made great contribution to the overall enhancement of hardness as shown in Table 1. The TEM analysis on these ultrafine matrix precipitates is currently in progress.

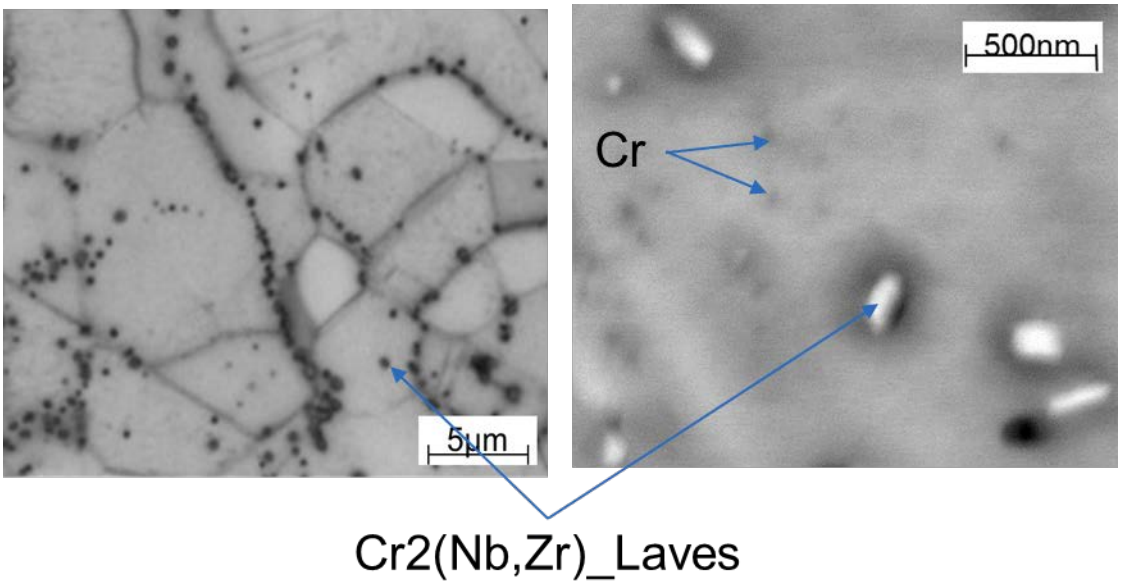

Figure 4. Comparison optical image with SEM BSE image showing a bimodal distribution of precipitates in CCNZA5 samples.

Future work

1) Complete TEM characterization of fine and ultrafine precipitates, and measure the tensile properties of the CCNZA5 and CCNZ5B samples between room temperature and 500°C.
2) Continue experimental study of the additional designed model alloys (based on insight obtained from the TEM and tensile characterization of the initial Cu alloy heats).
3) Perform thermodynamic calculations on the Cu-Cr-Ta-Zr system to explore the potential to achieve reduced activation high-performance Cu alloy for high heat flux substrates.

References

[1] D. Stork, P. Agostini, J.L. Boutard, D. Buckthorpe, E. Diegele, S.L. Dudarev, C. English, G. Federici, M.R. Gilbert, S. Gonzalez, A. Ibarra, C. Linsmeier, A. Li Puma, G. Marbach, P.F. Morris, L.W. Packer, B. Raj, M. Rieth, M.Q. Tran, D.J. Ward, S.J. Zinkle, J. Nucl. Mater., 455 (2014) 277-291.
[2] S.J. Zinkle, Phys. Scr., T167 (2016) 014004.
[3] K.R. Anderson, J.R. Groza, Metall. Mater. Trans. A 32 (2001) 1211.
[4] J.R. Groza, J.C. Gibeling, Mater. Sci. Eng. A171 (1993) 115.
[5] C. Sauer, et al., Int. J. Powder Metall. 33 (1997) 45.
[6] C. Sauer, et al., Z. Metallkunde 89 (1998) 119.
[7] S.J. Zinkle, L.L. Snead, Annu. Rev. Mater. Res. 44 (2014) 241.